

## Design and Evaluation of Dual Release from Anacardic Acid-Based Polyurea Nanocapsules Components

Sâmeque N. Oliveira,<sup>a,b,c</sup> Antonia F. J. Uchoa,<sup>b</sup> Denise R. Moreira,<sup>b</sup> Cesar L. Petzhold,<sup>d</sup> Clemens K. Weiss,<sup>e</sup> Katharina Landfester<sup>c</sup> and Nágila M. P. S. Ricardo<sup>ib\*,b</sup>

<sup>a</sup>Instituto Federal do Ceará, Campus Boa Viagem, 63870-000 Boa Viagem-CE, Brazil

<sup>b</sup>Departamento de Química Orgânica e Inorgânica, Centro de Ciências, Campus do Pici, Universidade Federal do Ceará, 60455-760 Fortaleza-CE, Brazil

<sup>c</sup>Max Planck Institute for Polymer Research, Ackermannweg 10, 55128 Mainz, Germany

<sup>d</sup>Departamento de Química Orgânica, Instituto de Química, Universidade Federal do Rio Grande do Sul, 91501-970 Porto Alegre-RS, Brazil

<sup>e</sup>University of Applied Science Bingen, Berlinstrasse 109, 55411 Bingen, Germany

Anacardic acid (AA) is a bioactive phytochemical found in the nutshell of *Anacardium occidentale*, a tropical plant originally from Brazil. In this work, cross-linked anacardic acid nanocapsules (NC) were obtained by interfacial polymerization carried out using the inverse miniemulsion technique with 2,4-toluene diisocyanate (TDI). For this purpose, a functionalized monomer from AA was synthesized for formation of lipase-cleavable ester linkages by coupling of amino acids. The synthesis was planned so that when these ester linkages get exposed to an enzyme, they are broken down and released AA. Furthermore, the N-termini of the coupled amino compounds were used as sites for the polyaddition with TDI at the droplet interface in the inverse miniemulsion. The permeability of the shell was studied on the fluorescent dye, sulforhodamine 101 (SR101), using fluorescence spectroscopy. After redispersion in water, the enzymatic cleavage of NC and the release of the SR101 were both monitored in real time. The released AA was proven to be active *in vitro* against *Bacillus subtilis* colonies in the bacterial tests. The results indicate that the use of NC is a promising strategy, which can make feasible the application of AA for therapeutic purposes and as nanocarriers for the delivery of active components.

**Keywords:** anacardic acid, inverse miniemulsion, polyurea, nanocapsule, antibacterial activity

### Introduction

Anacardic acid (AA) is a phenolic constituent present in cashew nut liquid (CNSL) and a renewable resource of immense potential. It is a mixture of several closely related organic compounds each consisting of a salicylic acid substituted with aliphatic chains of different unsaturation degree, as shown in Figure 1.

AA shows antioxidant activity preventing the generation of superoxide radicals by inhibiting xanthine oxidase,<sup>1</sup> and has also been found to be a lipoxygenase inhibitor.<sup>2</sup> Additionally, AA has been proposed to be a useful chemoprotectant<sup>3</sup> and furthermore capable of protecting

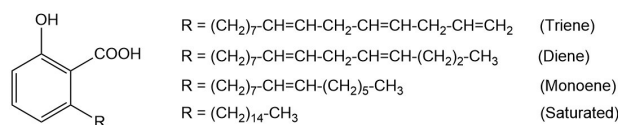


**Figure 1.** Structures of anacardic acid mixture.

human cells from oxidative stress and providing a gastroprotective effect from ethanol induced damage.<sup>4</sup> Some studies have also shown that AA can be used as a promising agent in the treatment of rheumatoid arthritis<sup>5</sup> and exhibits anticonvulsive properties as a neuroprotective compound.<sup>6</sup>

The bactericidal properties of AA have been shown on *Propionibacterium acnes*, *Corynebacterium xerosis*, *Streptococcus mutans*,<sup>7</sup> and also on methicillin resistant *Staphylococcus aureus* (MRSA)<sup>8</sup> that has become a

\*e-mail: naricard@ufc.br

Editor handled this article: Fernando C. Giacomelli (Associate)

significant threat to public health due to its increased virulence and resistance to an increasingly broad spectrum of antibiotics. In addition, AA also exhibits bactericidal properties on *Helicobacter pylori* (*H. pylori*),<sup>9</sup> a species of bacterium which infects the stomach and duodenal mucosa responsible for gastritis, ulcers and increases the stomach cancer incidence.<sup>10</sup> Moreover, AA could be a potent target molecule like a therapeutic agent in the treatment of cancer.<sup>11-16</sup> A study<sup>17</sup> also has associated the anacardic acid supplementation with a potential protective role on oxidative and inflammatory mechanisms in the lungs. Furthermore, a study<sup>18</sup> has investigated photoprotective and anti-inflammatory activities of AA in human skin. Recently, other studies<sup>19,20</sup> indicated that the anacardic acid inhibit severe acute respiratory syndrome coronavirus 2 (SARS-CoV-2) replication *in vitro* at nontoxic concentrations. The results provide a novel natural product as promising SARS-CoV-2 antiviral.<sup>19,20</sup>

Polymer nanoparticles have become highly promising candidates for the transport and release of drugs mainly because they provide means for delivering active molecules in controlled time and site specifically.<sup>21-23</sup> Several works<sup>24-28</sup> have been developed in the preparation of polymeric nanoparticles via miniemulsion. Therefore, we want to make use of this option to protect AA against degradation during transport in the body, to release it in its specific sites of action and to sustain and enhance its pharmacological/biological effect. Accordingly, the miniemulsion polymerization has been proven a technique highly adaptable to the preparation of nanoparticles as complex carriers to attain these characteristics.<sup>22,29</sup> The inverse miniemulsion polymerization has been used to synthesize polyurethane and polyurea nanocapsules by interfacial polyaddition<sup>30</sup> to encapsulate water-soluble dyes, contrast agents<sup>31,32</sup> and drugs<sup>33,34</sup> which could be liberated triggered by a variety of stimuli, such as pH, temperature, light and the presence of enzymes.<sup>35</sup> Enzyme triggered shell degradation and payload release has been realized by introducing peptide segments in the shell.<sup>36</sup> Hyaluronic acid-based nanocapsules allowed the enzymatic cleavage in the presence of bacteria and led to the release of polyhexanide in order to prevent bactericidal infection.<sup>37</sup> In the case of dexamethasone capsules, the polymerized drug itself formed the shell and became active upon degradation.<sup>38</sup>

The aim of this work was to prepare polyurea nanocapsules via interfacial polyaddition from the synthesis of a functionalized anacardic acid monomer. These nanocapsules have specific enzymatically triggered release properties which result in the release of AA in its free form. This characteristic was designed so that we could take advantage of the biological and pharmacological properties during the cleavage of the nanocapsules as a

prolonged release delivery system and protecting AA from degradation by transferring it into a polymer.

## Experimental

### Materials

Anacardic acid (AA) was extracted from cashew (*Anacardium occidentale* L.) nutshell liquid (CNSL) according to the method described by Paramashivappa *et al.*<sup>39</sup> For the extraction and purification of AA, all solvents had HPLC (high performance liquid chromatography) grade. Hexane (95.0%, Fisher, Mainz, Germany), ethyl acetate (EtOAc, 99.8%, Sigma-Aldrich, Mainz, Germany), methanol (99.9%, ChromaSolv, Mainz, Germany), calcium hydroxide (96.0%, Fluka, Mainz, Germany), hydrochloric acid (37.0%, Sigma-Aldrich, Mainz, Germany) were used as supplied. For the HPLC analyses of anacardic acid, acetonitrile (99.9%, ChromaSolv, Mainz, Germany), deionized water (MilliQ<sup>®</sup>, Darmstadt, Germany) and acetic acid (99.0%, ReagentPlus, Mainz, Germany) were used in an 80:20:1 v/v as mobile phase. For the synthesis and purification of the monomer from anacardic acid, Fmoc-6-amino hexanoic acid (Fmoc-6-Ahx-OH) (97.0%, Novabiochem<sup>®</sup>, Mainz, Germany), 2-(Fmoc-amino) ethanol (97.0%, Sigma-Aldrich, Mainz, Germany), *N,N*-dimethylformamide (extra dry DMF, 99.8%, AcroSeal, Mainz, Germany), *N*-ethyl-diisopropylamine (DIEA, 98.0%, Fluka, Mainz, Germany), COMU<sup>®</sup> (97.0%, Sigma-Aldrich, Mainz, Germany), piperidine (99.5%, Alfa Aesar, Mainz, Germany), dichloromethane (CH<sub>2</sub>Cl<sub>2</sub>, 99.9%, Fisher Chemical, Mainz, Germany), and sodium bicarbonate (NaHCO<sub>3</sub>, 99.7%, Sigma-Aldrich, Mainz, Germany) were used as received. For the preparation and characterization of the nanocapsules, cyclohexane (99.5%, HiPerSolvChromanorm, Mainz, Germany), *N,N*-dimethylformamide (DMF, 98.0%, Sigma-Aldrich, Mainz, Germany), toluene 2,4-diisocyanate (TDI, 98.0%, Sigma-Aldrich, Mainz, Germany), crystalline anhydrous lithium bromide (LiBr, 99.0%, Alfa Aesar, Mainz, Germany), sodium dodecyl sulfate (SDS, 99.0%, Merck, Mainz, Germany), sulforhodamine 101 (SRS101, 95.0%, Sigma-Aldrich, Mainz, Germany), Amano lipase PS from *Pseudomonas cepacia* (Lipase PS, Sigma-Aldrich, Mainz, Germany), and ninhydrin (99.0%, PA, Fluka, Mainz, Germany) were used as supplied. In addition, the block copolymer emulsifier poly(butylene-*co*-ethylene)-block-poly(ethylene oxide) P(B/E-*b*-EO) consisting of a poly(butylene-*co*-ethylene) block (molecular weight ( $M_w$ ) = 3700 g mol<sup>-1</sup>) and a poly(ethylene oxide) block ( $M_w$  = 7300 g mol<sup>-1</sup>) was synthesized starting from

Kraton liquid (Shell, Wesseling, Germany), which was dissolved in toluene, by adding ethylene oxide under typical conditions of anionic polymerization according to the method described.<sup>40</sup> 0.1 M sodium phosphate buffer solution (PBS, pH = 7.4) was prepared mixing 0.1 M of sodium phosphate monobasic solution ( $\text{NaH}_2\text{PO}_4$ , 99.0%, Sigma-Aldrich, Mainz, Germany) and 0.1 M sodium phosphate dibasic solution ( $\text{Na}_2\text{HPO}_4$ , 99.0%, Sigma-Aldrich, Mainz, Germany).

#### Extraction of anacardic acid

The anacardic acid mixture was obtained using the methodology from the literature.<sup>39</sup> In brief, the separation from CNSL was carried out by precipitation of AA as calcium salt, without the toxic phenolic material. Subsequently, AA was regenerated via acid hydrolysis (Figure S1, Supplementary Information (SI) section). The identity of anacardic acid was analyzed by HPLC revealing that the extract contained mostly triene, diene, and monoene forms of the aliphatic side chain, in accordance with other studies.<sup>41</sup>

#### Synthesis of functionalized monomer from anacardic acid

The synthesis consisted of the formation of lipase-cleavable ester linkages by coupling an amino acid (Fmoc-6-Ahx-OH) and amino ethanol (2-(Fmoc-amino) ethanol) to anacardic acid. The reactions were carried out at room temperature using the peptide coupling reagent COMU in the presence of organic base DIEA via three steps, in

accordance to Figure 2: (i) coupling of Fmoc-6Ahx-OH to the hydroxyl group present on anacardic acid (1) to obtain of compound 2; (ii) coupling of 2-(Fmoc-amino) ethanol to the carboxylic group present on anacardic acid for formation of compound 3 and (iii) deprotection of the amino acids with the removal of the Fmoc groups to obtain the monomer (4). In the last step of the synthesis, the product was deprotected and purified to give the functionalized monomer from anacardic acid. Fmoc protecting group had been used for side chain protection and was removed by 20% piperidine in DMF.<sup>42</sup> Detailed information on the synthesis and characterization is available in the SI section.

The synthesis strategy of monomer was planned with a view to the N-termini of the coupled amino compounds were used as sites for the polyaddition with diisocyanate at the droplet interface in the inverse miniemulsion as presented in the Figure 3. The generated polyurea forms the shell of nanocapsule consisting of monomer crosslinked with 2,4-toluene diisocyanate (TDI).

#### Procedure for polymerization via inverse miniemulsion

The monomer (4.20 mg) was dissolved in 300 mg *N,N*-dimethylformamide (DMF) containing 5 g L<sup>-1</sup> LiBr as osmotic pressure agent. Then, the continuous phase, consisting of a 0.5 wt.% P(E/B-b EO) solution in 2.8 g cyclohexane, was added and the mixture was stirred at room temperature at 1400 rpm for 10 min. Subsequently, the dispersion was sonicated at 70% of amplitude (Branson Sonifier D450, Massachusetts, United States, 1/8" tip, ice

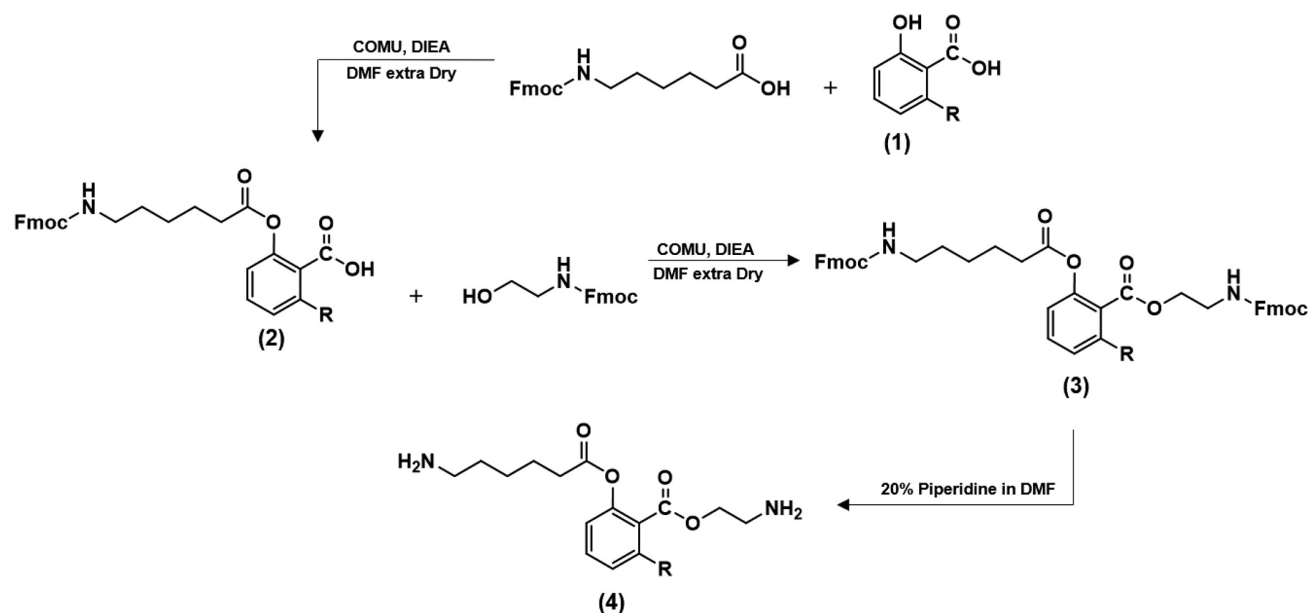


**Figure 2.** Synthetic route and reaction conditions for the preparation of functional monomer (4) from anacardic acid (1). All reactions were carried out at room temperature.

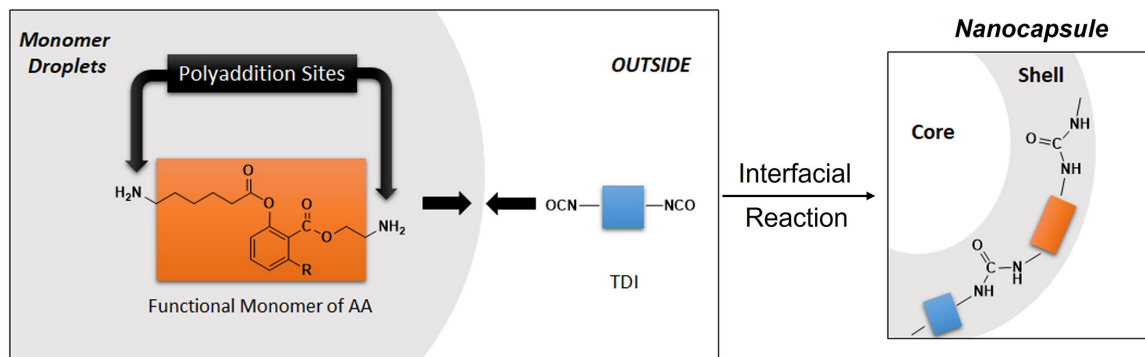


**Figure 3.** Schematic representation of the interfacial polyaddition between NCO groups from TDI and NH<sub>2</sub> groups from monomer (the orange and blue rectangles represent part of the monomer and TDI molecules, respectively).

cooling), for 3 min total sonication time with 10 s pulse/10 s pause. A freshly prepared TDI (TDI 1:1 and 1:2, with respect to the molar ratio of amino groups of the monomer) in cyclohexane (200 mg) solution was added drop wise. The mixture was stirred for 18 h. Then, the miniemulsion was redispersed in twice its weight of aqueous 0.3 wt.% sodium dodecyl sulfate (SDS) solution until complete cyclohexane evaporation at 40 °C under strong magnetic stirring, followed by mild ultrasonification (3 min total, applied in pulses of 10 s with 10 s pause, 30% intensity, 1/8" tip) to avoid flocculation. Samples were then dialyzed in approximately 2 L of deionized water (dialysis cassettes, cut-off 10 kDa) for a week, with daily exchange to reduce the amount of surfactants (SDS and P(E/B- b-EO), to eliminate present DMF and to remove monomer-free molecules, not covalently bound to the nanocapsules (NC). After transferring the nanocapsules in water a stable dispersion was generated. Simultaneously, the permeability of NC shells for the encapsulation of a small hydrophilic molecule was investigated with the encapsulated water-soluble dye (sulforhodamine 101).

#### Preparation of nanocapsules

The procedure used for the synthesis of nanocapsules was based on an already established protocol<sup>36</sup> for the preparation of polyurea nanocapsules via inverse miniemulsion. Two different ratios of the NCO groups of the toluene 2,4-diisocyanate (TDI) to the amino groups of the monomer were used for polymerization: (i) 1:1 (1 mol eq. TDI) and (ii) 2:1 (2 mol eq. TDI). After the synthesis of the nanocapsules in cyclohexane, the polyurea nanocapsules were transferred to an aqueous SDS solution. Note that the block copolymer P(E/B-b-EO) is an effective surfactant for a water-in-oil system, whereas a water-soluble surfactant is required for the stabilization of the nanocapsules in aqueous medium.

#### Procedure for preparation of nanocapsules with dye

The nanocapsules containing sulforhodamine 101 were prepared in the same way as described above, with composition of the mixture containing the monomer (4.50 mg) and SR101 (2 mg) dissolved in 750 mg *N,N*-dimethylformamide (DMF) and 5 g L<sup>-1</sup> LiBr as osmotic pressure agent.

#### Enzymatic cleavage/degradation assays of the nanocapsules with dye

The cleavage experiments were carried out by diluting the dispersion five times in water and adding lipase PS (final concentration of 5 mg mL<sup>-1</sup>). In each case, a control experiment was prepared from the same sample under the same conditions but without the addition of enzyme. The fluorescence intensities were monitored using a Tecan M1000 microplate reader at 37 °C and the wavelengths ( $\lambda$ ) used for the fluorescent dye (SRS 101) were  $\lambda_{\text{ex}} = 580$  nm (excitation) and  $\lambda_{\text{em}} = 605$  nm (emission) with 5 nm bandwidth. The measurements were conducted every minute and the plate was briefly shaken (5 s) before each recording. Each data point corresponds to the average value of eight replicates.

#### Monitoring of anacardic acid release in degradation assays

The degradation assays were carried out by diluting the dispersion five times in 0.1 mol L<sup>-1</sup> phosphate buffer and adding lipase PS to a final concentration of 5 mg mL<sup>-1</sup>. In each case, a control experiment was prepared from the same sample under same conditions but without the addition of the enzyme. The mixture was maintained under constant agitation at 400 rpm during the assays. The anacardic acid liberated was quantitatively monitored by high performance liquid chromatography (HPLC).

## Characterization

HPLC was carried out using a Shimadzu SPD-10VP chromatograph, UV-Vis detector, which utilized a C-18 analytical column (25 cm × 4 mm) from Supelco® and a LC-10AT pump (Massachusetts, United States). The mobile phase consisted of acetonitrile/water/acetic acid (80:20:1), which was run in the isocratic mode phase at a wavelength of 280 nm. <sup>1</sup>H and <sup>13</sup>C nuclear magnetic resonance (NMR) spectra were recorded on an Avance 300 MHz NMR spectrometer (Bruker Bioscience, Billerica, Massachusetts, United States) at 298.7 K, using CDCl<sub>3</sub> (99.96 atom% D, Sigma-Aldrich, Darmstadt, Germany) as solvent. Samples for size exclusion chromatography (SEC) were prepared at 1 g L<sup>-1</sup> in DMF. The sample injection was performed by a 717 plus auto sampler (water) at 60 °C (DMF) with flow as 1 mL min<sup>-1</sup>. Three GRAM columns (PSS), 300 × 80 mm, 10 μm particle size with respective pore sizes of 106, 104, and 103 Å were employed. Particle sizes and size distributions (average value from n = 10) were determined by DLS (dynamic light scattering) with PCCS (photon cross-correlation spectroscopy) in a Nanophox particle analyzer, Sympatec GmbH, Germany. Zeta potential measurements (n = 10) were performed using a Zetasizer Nano Z equipment (Malvern, Mainz, Germany). The nanoparticle dispersion was added to a solution of 10<sup>-3</sup> mol L<sup>-1</sup> KCl and the final values are presented as mean of 10 replicates accompanied by the standard deviation. Scanning electron micrographs studies were carried out on a Gemini 1530 (Carl Zeiss AG, Darmstadt, Germany) with an In-Lens detector and acceleration voltages between 0.2-0.3 kV. Briefly, the samples were prepared by drop casting 5 μL of diluted dispersions in cyclohexane and water on a silicon wafer. Transmission electron microscopy (TEM) pictures were taken on a FEI Tecnai F20 (Darmstadt, Germany) microscope under an acceleration voltage of 200 kV. The samples were prepared with 5 μL of diluted dispersion placed on a 300 mesh carbon-coated copper grid. The average diameter of the NCs was determined by encircling the NCs in the TEM images and transforming the irregularly-shaped area of each grain into a circle with equivalent surface area (between 100 and 150 NCs were measured). The particle size analyses were measured using ImageJ software,<sup>43</sup> which is a public domain Java image processing computer program. Fluorescence intensity measurements (n = 10) were performed with Tecan® Infinite M1000 PRO Microplate Reader. The FTIR spectroscopy analyses were performed on a PerkinElmer Spectrum BX FT-IR spectrometer (PerkinElmer, Shelton, CT, USA). The range of the wavelength was between 4000 and 400 cm<sup>-1</sup>. For solid samples, 3 mg of the nanocapsules were mixed with KBr, pressed and subsequently measured.

## Tests for bacterial activity

Antibacterial activity was tested on *Bacillus subtilis* cultures. Pre-incubated *Bacillus subtilis* cultures were placed on Agar plates. The bacteria were grown in culture medium and diluted in 10 mL PBS to achieve approx. 500 colony-forming unit (CFU) on the plate. A dispersion of AA containing nanocapsules was diluted to concentrations of 1 and 5 mg L<sup>-1</sup>, respectively. 200 μL of these dispersions were added to the Agar plate after adding the bacteria dispersion. Controls with water and AA in DMSO, respectively, were also prepared. DMSO and water (negative control group) did not exhibit any antibacterial activity as shown in SI section. All plates were incubated for 16 h at 30 °C.

## Results and Discussion

### Characterization and synthesis of monomer from anacardic acid

The modification of anacardic acid was carried out by coupling of Fmoc-protected amino acids. As coupling agent, COMU<sup>44</sup> was used for activation of the carboxylic group to the coupling reaction. It allows the formation of ester linkages efficiently at room temperature.<sup>45</sup> The first coupling consisted of activating the carboxyl group from Fmoc-6-Ahx-OH for the formation of an ester bond with hydroxyl groups from anacardic acid (Figure 2, compound 2). In the second coupling step, the carboxylic group from anacardic acid was activated in order to form the ester bond with the hydroxyl from 2-(Fmoc-amino) ethanol (Figure 2, compound 3). In the last step, Fmoc amino-protecting groups were removed to obtain free amine on the monomer (Figure 2, monomer, compound 4). Thereby, piperidin (20% in DMF) is the routine reagent since Fmoc is cleaved swiftly under basic conditions.<sup>46</sup> The <sup>1</sup>H NMR spectra showed signals relating to the chemical structure of monomer, with chemical shifts between 3.0 to 3.7 ppm relative to the hydrogens of the carbons attached to the ester and amine groups from of coupled amino acids. The infrared (IR) spectra show bands attributed to the axial deformation of the aromatic CH for both anacardic acid (3010 cm<sup>-1</sup>) and the monomer (3007 cm<sup>-1</sup>), indicating that reactions have not occurred at the aromatic system (see SI section for details; Figures S6 and S7). Furthermore, the axial deformation of the C=C bonds are observed in both the anacardic acid (1647 cm<sup>-1</sup>) and the monomer (1654 cm<sup>-1</sup>) spectrum according to the unsaturations in the side chain C<sub>15</sub>H<sub>31-n</sub> (n = 2, 4 and 6). The monomer spectrum showed bands related to the ester axial asymmetrical deformation at 1380 cm<sup>-1</sup> (C-C(=O)-O)

and  $1118\text{ cm}^{-1}$  (O–C–O).<sup>47</sup> A strong band was also observed at  $1589\text{ cm}^{-1}$ , which can probably be associated to the vibrations of axial deformation at primary aliphatic diamines. In addition, the positive ninhydrin test indicated the existence of primary amines.

#### Characterization of colloidal properties of dispersion and nanocapsules

In order to verify if the polymerization reaction was successful, gel permeation chromatography (GPC) analysis was performed. GPC chromatograms were obtained by wavelength monitoring at  $\lambda = 270\text{ nm}$ , which allowed selective detection of the products and the TDI (absorbance of the aromatic groups) and did not interfere with the P(E/B-b-EO) surfactant since it does not exhibit aromatic groups. Figure 4 shows the chromatograms superimposed of the monomer (MAc) and of the miniemulsions prepared with 1 eq. TDI or 2 eq. TDI, lyophilized after the polyaddition.

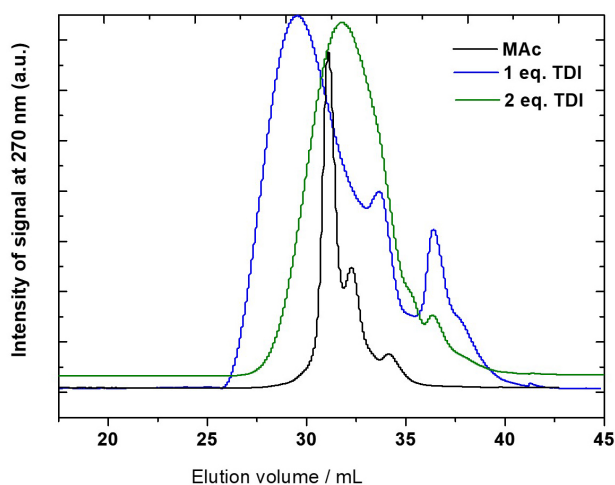


**Figure 4.** Chromatograms of GPC obtained for the miniemulsions prepared in the two equivalents of TDI (1 eq. TDI and 2 eq. TDI) in comparison to the monomer.

The obtained chromatograms indicated the polymerization for the two miniemulsion systems (1 eq. TDI and 2 eq. TDI), with a higher degree of polymerization for the miniemulsion with 1 eq. TDI, with a marked change towards volumes of elution, in other words for higher molecular weights. This result was verified by the relative mean molar mass ( $M_w$ ) and mean number of molar mass ( $M_n$ ) values for the samples presented in Table 1. No significant variation in the molar mass after redispersion in water is observed for the miniemulsion prepared with 1 eq. of TDI, the opposite is shown for the miniemulsion prepared with 2 eq. of TDI. This may be related to side reactions caused by excess TDI in the presence of water, forming carbamic acid which, by decarboxylation, generates new amines. These, in turn, react with free TDI molecules forming other urea bonds contributing to the increase in molar mass.

The analysis by infrared spectroscopy is also useful, providing information regarding the reaction of the isocyanate group and estimating the polyurea bonds formed in the polymerization. Figure 5 shows the overlap of Fourier transform infrared (FTIR) spectra for the lyophilized nanocapsule samples before and after redispersion in water for the two miniemulsion systems as compared to the monomer (MAc). The spectra show a strong band between  $3450$  and  $3200\text{ cm}^{-1}$ , corresponding generally to the combination of the N–H stretching vibrational bands in amine or imine groups of polyurea.<sup>30</sup> As well, absorption bands between  $2950$  and  $2750\text{ cm}^{-1}$  related to the stretching vibrational bands of C–H in CH, CH<sub>2</sub> and CH<sub>3</sub> groups.

Moreover, from the absence of the characteristic band of the  $\text{–N=C=O}$  around  $2270\text{ cm}^{-1}$ , complete conversion of TDI in the miniemulsion prepared with 1 eq. TDI can be concluded (Figure 5a). This band, in contrast, appears very pronounced in the miniemulsion prepared with 2 eq. TDI in cyclohexane (Figure 5b), but is not observed in the

**Table 1.** Results obtained by GPC for the relative mean values ( $n = 3$ ) of the weight average molar mass ( $M_w$ ), the number average molar mass ( $M_n$ ) and the polydispersion index ( $PI = M_w/M_n$ ) using ultraviolet detectors (UV) and refractive index and DMF as diluent for nanocapsules with and without encapsulated SR101 dye

TDI equivalents of the sample	Dispersed phase	$M_w / (\text{g mol}^{-1})$		$M_n / (\text{g mol}^{-1})$		PI	
		UV	RI	UV	RI	UV	RI
1 eq. TDI	cyclohexane	10700	9700	4300	3400	2.5	2.8
	water	12900	11700	7300	6500	1.7	1.8
2 eq. TDI	cyclohexane	5200	5100	2900	2600	1.8	1.9
	water	12700	12000	7300	6700	1.7	1.7
1 eq. TDI with SR101	cyclohexane	12200	9900	4000	2500	3.0	3.8
	water	14800	16200	8300	8000	1.7	2.0
2 eq. TDI with SR101	cyclohexane	3500	3300	2100	1800	1.6	1.8

TDI: 2,4-toluene diisocyanate;  $M_w$ : weight average molar mass;  $M_n$ : number average molar mass; PI: polydispersion index ( $PI = M_w/M_n$ ); UV: ultraviolet; RI: refractive index; SR 101: sulforhodamine 101.

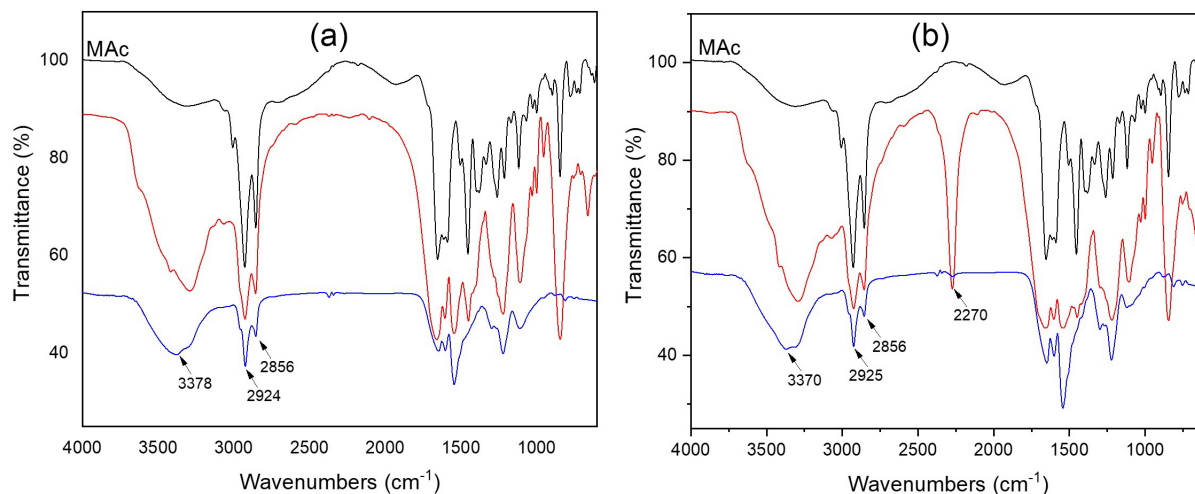


**Figure 5.** FTIR (KBr) spectra obtained for the MAc (black) and for the NCs in cyclohexane (red) and water (blue) synthesized using 1 eq. of TDI (a) and 2 eq. of TDI (b).

spectra referring to NCs after their transfer to water (in blue in Figure 5b) indicating that excess TDI has promoted hydrolysis reaction between the isocyanate groups and water molecules. Measurements from photon cross correlation spectroscopy (PCCS) (Table 2) show a narrow nanocapsule size distribution for the two prepared miniemulsion systems. In both, the values are centered around 200 nm when the original nanocapsules are dispersed in cyclohexane, whereas, after transfer to the water phase, these values are increased to a range between 300 and 400 nm. This increase may be related to the diffusion of water into the NCs and, consequently, an increase in its size.<sup>37</sup> The similarity between the values found for the NC size in the two systems can be understood by the fact that, except for the difference in TDI equivalence, all other procedures and reagents involved in the synthesis were the same.

As is reported, essential factors in determining the size of the nanocapsules are the polarity of the solvents in each phase, the proportion between the phases and the nature and

concentration of the surfactants used.<sup>48,49</sup> In addition, the control of the mean diameter of the NCs can be achieved by the intensity and duration of homogenization.<sup>50-52</sup> The similarity of size between the nanocapsules using different amounts of TDI was also demonstrated by other works with miniemulsion polyaddition systems, where the size of the nanocapsules was unchanged by increasing amounts of TDI, while the thickness of the capsules slightly increased.<sup>31</sup> The zeta potential values  $> +25$  mV or  $< -25$  mV usually have high degree of stability.<sup>53</sup> According to the zeta potential values (Table 2), the nanocapsules presented a good stability.<sup>53</sup>

The morphology of the nanocapsules was examined from TEM. In addition to the confirmation of polymerization, the micrographs also provide structural information on the synthesized NCs (Figures 6 and S10 of SI section). The micrograph shown in Figure 6 shows nanocapsules with sizes smaller than those obtained by PCCS, as summarized in the Table 2. These lower values are probably due to the

**Table 2.** Particle size (determined by PCCS and TEM) and zeta potential determined for the nanocapsules in the different media (and with or without encapsulated SR101)

TDI equivalents of the sample	Dispersed phase	Particle size PCCS / nm	Particle size TEM / nm	Zeta potential / mV
1 eq. TDI	cyclohexane	216 ± 9	71 ± 29	–
	water	327 ± 25	102 ± 34	–41
2 eq. TDI	cyclohexane	244 ± 7	286 ± 23	–
	water	410 ± 21	292 ± 56	–25
1 eq. TDI, SR101	cyclohexane	187 ± 4	128 ± 23	–
	water	310 ± 17	250 ± 53	–34
2 eq. TDI, SR101	cyclohexane	265 ± 59	325 ± 67	–
	water	582 ± 153	389 ± 15	–43

TDI: 2,4-toluene diisocyanate; PCCS: photon cross-correlation spectroscopy; TEM: transmission electron microscopy; SR 101: sulforhodamine 101.

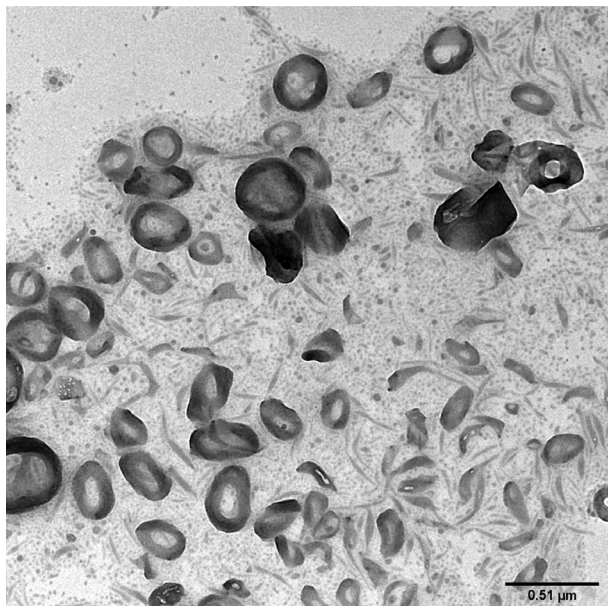


**Figure 6.** TEM micrograph obtained for the nanocapsules synthesized in cyclohexane and redispersed in water.

collapse effect of the nanocapsules observed in the images, because of the freeze-drying of the samples and to the vacuum conditions under evaluation. TEM confirmed the polymerization and the formation of the nanocapsules.

#### Enzymatic cleavage experiments

For the enzymatic cleavage experiment, nanocapsules containing encapsulated dye sulforhodamine 101 (SR101) were prepared. SR101 is a fluorescent dye widely used as a contrast in neurophysiological experiments for the analysis of healthy brain cells.<sup>54-56</sup> In the present work, it was used to monitor the degradation of nanocapsules during the enzymatic cleavage assays, as in other studies.<sup>31,36</sup> The sulforhodamine did not change the nanocapsule formation (see Tables 1 and 2). Fluorescence spectroscopy was used to monitor the emission of SR101 after liberation from the nanocapsules, because of enzymatic shell degradation. An illustrative scheme for the enzymatic cleavage of the

nanocapsules and the release of the SR101 fluorescent dye is shown in Figure 7.

*In vitro* degradation assays were performed for the encapsulated dye nanocapsules dispersed in phosphate buffer solution (pH = 7.4) and in the presence of the enzyme Lipase PS (*Pseudomonas cepacia*), whereas the control group consisted of assays in the same conditions but in the absence of the enzyme. The lipase PS from *Pseudomonas cepacia* presents high specificity in the hydrolysis of ester bonds, reason for choice to carry out the tests. During the monitoring of the enzyme treatment of the NCs (Figure S12 in SI section) the increase of fluorescence signal intensity was observed for 40 h for the miniemulsion prepared with 2 eq. of TDI, while 48 h for the miniemulsion prepared with 1 eq. of TDI. The increasing signal is a clear indication for the release of the initially encapsulated dye. From these times no considerable variation of the signal was observed for both samples, indicating the time limit of degradation of the NCs.

The progressive degradation on the surface of the NCs makes available more polyurea ester bonds for degradation. This can be observed by the shape of the degradation curves, where in the initial range there is an exponential increase of the signal up to a maximum value. It is possible that this maximum time reached is smaller for the miniemulsions prepared with 2 eq. of TDI due to the fact that the nanocapsules in these miniemulsions present a thicker polymer layer and thus more ester bonds available, reducing the total degradation time compared to that presented by the miniemulsions with 1 eq. of TDI.

Degradation assays were performed with the dye-free nanocapsules in order to monitor the release kinetics of anacardic acid. Samples were collected during the degradation assays at periods of 6, 12, 24 and 48 h and analyzed in HPLC for the quantification of released anacardic acid. The chromatograms obtained for the samples and for the control groups are shown in Figure S13 (SI section). From the chromatograms obtained the release of anacardic acid in its free form

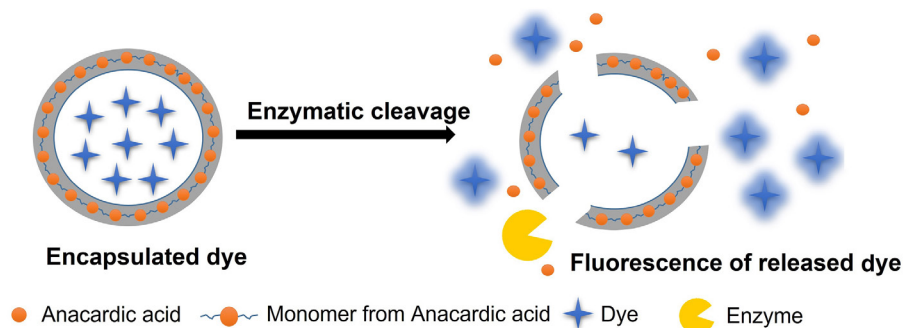


**Figure 7.** Illustrative scheme for enzymatic degradation of the polymeric shell of the NCs with encapsulated dye demonstrating the regeneration of the anacardic acid and fluorescent activity of the dye as it is released.

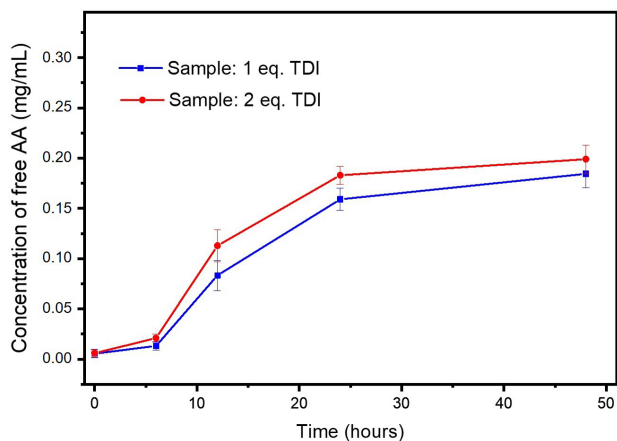


**Figure 8.** Time dependent concentration of anacardic acid during enzymatic degradation (mean and 95% confidence intervals derived from  $n = 3$ ).

for the samples was quantified. A graph with the kinetic release profile corresponding to the miniemulsions prepared with the different molar equivalents of the TDI (1 eq. TDI and 2 eq. TDI) is shown in Figure 8 (see also Table S1 in SI section).

The chromatograms of the degradation of the nanocapsules showed predominance of the side chain anacardic acid containing three double bonds. The results obtained in this study were similar to those observed in other studies,<sup>39</sup> which was also found to be more abundant in the AA mixture obtained from cashew nuts. The assays confirmed the effectiveness of lipase enzyme activity in cleavage of nanocapsules and release of anacardic acid. The two prepared samples of the nanocapsules (1 eq. TDI and 2 eq. TDI) showed similar release profile, with no significant variation in AA concentration observed between 24 and 48 h of assay. Additionally, from the theoretical content of anacardic acid present in the samples and comparing to the values quantified in the degradation tests, showed a 96 and 100% efficiency in the degradation of the prepared nanocapsules to 1 eq. TDI and 2 eq. TDI, respectively. These results can be related to the fluorescence date. Within the first few hours, bonds are broken, the shell becomes leaky and the encapsulated dye is released, while still polymer/oligomers remain intact and therefore only few free AA can be detected. After 7 h AA becomes liberated, a plateau is reached after about 24 h, which is the onset of the fluorescence plateau.

#### Bacterial tests

Antibacterial activity could be shown by treating *Bacillus subtilis* colonies with nanocapsule dispersions. Figure 9 shows agar plates incubated with *Bacillus subtilis* and nanocapsule dispersions in two different concentrations

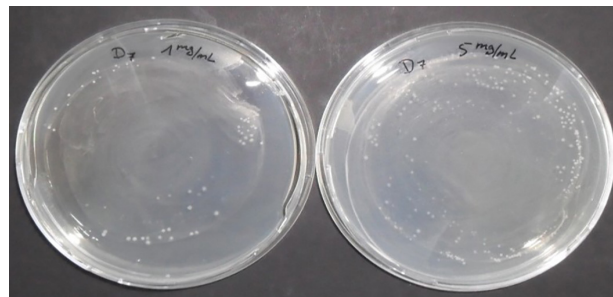


**Figure 9.** *Bacillus subtilis* on agar plates treated incubated with nanocapsule dispersion in two different concentrations: 200  $\mu\text{L}$  of 1 (left) and 5 (right)  $\text{mg L}^{-1}$ .

(1 and 5  $\text{mg L}^{-1}$ ) and control groups (Figure S14 in SI section). Although bacterial growth is not completely inhibited, far less bacterial colonies are visible after nanocapsules treatment, than without.

## Conclusions

In this work, a strategy was developed for the formation of polyurea nanocapsules consisting of a shell derived from anacardic acid and a core with a second component to take advantage of delivering both, anacardic acid and the encapsulated component at the area of interest. It could be shown that the enzymatic activity of lipase depolymerizes the shell and liberates the anacardic acid while at the same time releasing components encapsulated in the core of the nanocapsules. The inverse miniemulsion process was used to prepare the nanocapsules via interfacial polyaddition. The efficiency of the nanocapsules of releasing anacardic acid results indicate that the use of nanocapsules is a promising strategy, which will allow the co-delivery of anacardic acid and other active components at the same time for therapeutic purposes.

## Supplementary Information

Supplementary information is available free of charge at <http://jbcs.sbc.org.br> as PDF file.

## Acknowledgments

This study was partially supported by the Coordenação de Aperfeiçoamento de Pessoal de Nível Superior - Brasil (CAPES) - Finance Code 001 (PROEX 23038.000509/2020-82), Conselho Nacional de Desenvolvimento Científico e Tecnológico (CNPq), and CAPES (S.N.Oliveira). The authors thank Central Analítica UFC/CT-INFRA/MCTI-SISNANO/CAPES for the support. The corresponding author thanks CNPq for the research grant (N.M.P.S.R No. 309795/2021-4).

## Author Contributions

Sâmeque do N. Oliveira was responsible for investigation, formal analysis, writing original draft and editing; Antonia F. J. Uchoa for data curation and writing-review; Denise R. Moreira for data curation and writing-review; Cesar L. Petzhold investigation and writing-review; Clemens K. Weiss for project administration; Katharina Landfester for conceptualization, funding acquisition, and writing-review and editing; Nágila M. P. S. Ricardo for project administration, writing-review and editing, and funding acquisition.

## References

- Kubo, I.; Masuoka, N.; Ha, T. J.; Tsujimoto, K.; *Food Chem.* **2006**, *99*, 555. [Crossref]
- Wisastra, R.; Ghizzoni, M.; Boltjes, A.; Haisma, H. J.; Dekker, F. J.; *Bioorg. Med. Chem.* **2012**, *20*, 5027. [Crossref]
- Trevisan, M. T. S.; Pfundstein, B.; Haubner, R.; Würtele, G.; Spiegelhalder, B.; Bartsch, H.; Owen, R. W.; *Food Chem. Toxicol.* **2006**, *44*, 188. [Crossref]
- Morais, T. C.; Pinto, N. B.; Carvalho, K. M. M. B.; Rios, J. B.; Ricardo, N. M. P. S.; Trevisan, M. T. S.; Rao, V. S.; Santos, F. A.; *Chem.-Biol. Interact.* **2010**, *183*, 264. [Crossref]
- Yang, G.-h.; Zhang, C.; Wang, N.; Meng, Y.; Wang, Y.-s.; *Cytokine* **2018**, *111*, 350. [Crossref]
- Gomes Jr., A. L.; Tchekalarova, J. D.; Atanasova, M.; Machado, K. C.; Rios, M. A. S.; Jardim, M. F. P.; Găman, M. A.; Găman, A. M.; Yele, S.; Shill, M. C.; Khan, I. N.; Islam, M. A.; Ali, E. S.; Mishra, S. K.; Islam, M. T.; Mubarak, M. S.; Lopes, L. S.; Melo-Cavalcante, A. A. C.; *Biomed. Pharmacother.* **2018**, *106*, 1686. [Crossref]
- Muroi, H.; Kubo, I.; *J. Agric. Food Chem.* **1993**, *41*, 1780. [Crossref]
- Kubo, I.; Nihei, K. I.; Tsujimoto, K.; *J. Agric. Food Chem.* **2003**, *51*, 7624. [Crossref]
- Castillo-Juárez, I.; Rivero-Cruz, F.; Celis, H.; Romero, I.; *J. Ethnopharmacol.* **2007**, *114*, 72. [Crossref]
- Strugatsky, D.; McNulty, R.; Munson, K.; Chen, C.-K.; Michael Soltis, S.; Sachs, G.; Luecke, H.; *Nature* **2013**, *493*, 255. [Crossref]
- Davidson, S. M.; Townsend, P. A.; Carroll, C.; Yurek-George, A.; Balasubramanyam, K.; Kundu, T. K.; Stephanou, A.; Packham, G.; Ganesan, A.; Latchman, D. S.; *ChemBioChem* **2005**, *6*, 162. [Crossref]
- Kishore, A. H.; Vedamurthy, B. M.; Mantelingu, K.; Agrawal, S.; Reddy, B. A. A.; Roy, S.; Rangappa, K. S.; Kundu, T. K.; *J. Med. Chem.* **2008**, *51*, 792. [Crossref]
- Schultz, D. J.; Wickramasinghe, N. S.; Ivanova, M. M.; Isaacs, S. M.; Dougherty, S. M.; Imbert-Fernandez, Y.; Cunningham, A. R.; Chen, C.; Klinge, C. M.; *Mol. Cancer Ther.* **2010**, *9*, 594. [Crossref]
- Sukumari-Ramesh, S.; Singh, N.; Jensen, M. A.; Dhandapani, K. M.; Vender, J. R.; *J. Neurosurg.* **2011**, *114*, 1681. [Crossref]
- Gnanaprakasam, J. N. R.; Estrada-Muñiz, E.; Vega, L.; *Int. Immunopharmacol.* **2015**, *29*, 808. [Crossref]
- Nambiar, J.; Bose, C.; Venugopal, M.; Banerji, A.; Patel, T. B.; Kumar, G. B.; Nair, B. G.; *Exp. Cell Res.* **2016**, *349*, 139. [Crossref]
- Carvalho, A. L. N.; Annoni, R.; Silva, P. R. P.; Borelli, P.; Fock, R. A.; Trevisan, M. T. S.; Mauad, T.; *J. Ethnopharmacol.* **2011**, *135*, 730. [Crossref]
- Kim, M. K.; Shin, M. H.; Kim, Y. K.; Kim, H. Y.; Lee, Y. R.; Lee, D. H.; Chung, J. H.; *J. Dermatol. Sci.* **2017**, *86*, 252. [Crossref]
- Chen, Z.; Cui, Q.; Cooper, L.; Zhang, P.; Lee, H.; Chen, Z.; Wang, Y.; Liu, X.; Rong, L.; Du, R.; *Cell Biosci.* **2021**, *11*, 45. [Crossref]
- Li, D.; Yan, G.; Zhou, W.; Si, S.; Liu, X.; Zhang, J.; Li, Y.; Chen, Y.; *Cell Biosci.* **2022**, *12*, 65. [Crossref]
- El-Say, K. M.; El-Sawy, H. S.; *Int. J. Pharm.* **2017**, *528*, 675. [Crossref]
- Gharieh, A.; Khoee, S.; Mahdavian, A. R.; *Adv. Colloid Interface Sci.* **2019**, *269*, 152. [Crossref]
- Crociani, L.; Ruggiero, L. In *Smart Nanocontainers*; Nguyen-Tri, P.; Do, T.-O.; Nguyen, T. A.; Elsevier Inc.: Amsterdam, 2020. [Crossref]
- Jia, J.; Yin, Y.; Liu, W.; Li, X.; Wang, C.; *J. Cleaner Prod.* **2020**, *265*, 121601. [Crossref]
- Zhang, Z.; Liu, F.; Lin, Y.; *Colloids Surf., A* **2020**, *603*, 125264. [Crossref]
- Gu, T.; Zhang, Y.; Khan, S. A.; Hatton, T. A.; *Colloids Interface Sci. Commun.* **2019**, *28*, 1. [Crossref]
- Wang, J.; Lu, C.; Liu, Y.; Wang, C.; Chu, F.; *Ind. Crops Prod.* **2018**, *124*, 244. [Crossref]
- Boscán, F.; Barandiaran, M. J.; Paulis, M.; *J. Ind. Eng. Chem.* **2018**, *58*, 1. [Crossref]
- Landfester, K.; *Angew. Chem., Int. Ed.* **2009**, *48*, 4488. [Crossref]
- Crespy, D.; Stark, M.; Hoffmann-Richter, C.; Ziener, U.; Landfester, K.; *Macromolecules* **2007**, *40*, 3122. [Crossref]
- Paiphansiri, U.; Dausend, J.; Musyanovych, A.; Mailänder, V.; Landfester, K.; *Macromol. Biosci.* **2009**, *9*, 575. [Crossref]
- Rosenbauer, E.-M.; Landfester, K.; Musyanovych, A.; *Langmuir* **2009**, *25*, 12084. [Crossref]
- Landfester, K.; Mailänder, V.; *Expert Opin. Drug Delivery* **2013**, *10*, 593. [Crossref]
- dos Santos, S. B. F.; Pereira, S. A.; Rodrigues, F. A. M.; da Silva, A. C. C.; de Almeida, R. R.; Sousa, A. C. C.; Fechine, L. M. U. D.; Denardin, J. C.; Aranedá, F.; Sá, L. G. A. V.; da Silva, C. R.; Nobre Júnior, H. V.; Ricardo, N. M. P. S.; *Int. J. Biol. Macromol.* **2020**, *164*, 2813. [Crossref]
- Rosenbauer, E. M.; Wagner, M.; Musyanovych, A.; Landfester, K.; *Macromolecules* **2010**, *43*, 5083. [Crossref]

36. Andrieu, J.; Kotman, N.; Maier, M.; Mailänder, V.; Strauss, W. S. L.; Weiss, C. K.; Landfester, K.; *Macromol. Rapid Commun.* **2012**, *33*, 248. [Crossref]
37. Baier, G.; Cavallaro, A.; Vasilev, K.; Mailänder, V.; Musyanovych, A.; Landfester, K.; *Biomacromolecules* **2013**, *14*, 1103. [Crossref]
38. Fichter, M.; Baier, G.; Dedters, M.; Pretsch, L.; Pietrzak-Nguyen, A.; Landfester, K.; Gehring, S.; *Nanomed. Nanotechnol., Biol. Med.* **2013**, *9*, 1223. [Crossref]
39. Paramashivappa, R.; Phani Kumar, P.; Vithayathil, P. J.; Srinivasa Rao, A.; *J. Agric. Food Chem.* **2001**, *49*, 2548. [Crossref]
40. Schlaad, H.; Kukula, H.; Rudloff, J.; Below, I.; *Macromolecules* **2001**, *100*, 4302. [Crossref]
41. Trevisan, M. T. S.; Ricarte, I.; dos Santos, S. J. M.; Almeida, W. P.; Ulrich, C. M.; Owen, R. W.; *Int. J. Food Prop.* **2018**, *21*, 921. [Crossref]
42. Isidro-Llobet, A.; Álvarez, M.; Albericio, F.; *Chem. Rev.* **2009**, *109*, 2455. [Crossref]
43. Rasband, W. S.; *ImageJ*, 1.51k; National Institutes of Health, USA, 2017.
44. El-Faham, A.; Albericio, F.; *J. Pept. Sci.* **2010**, *16*, 6. [Crossref]
45. Twibanire, J. D. A. K.; Grindley, T. B.; *Org. Lett.* **2011**, *13*, 2988. [Crossref]
46. Jones, J.; *Amino Acid and Peptide Synthesis*, vol. 7; Oxford University Press: Oxford, 2011.
47. Silverstein, R. M.; Webster, F. X.; Kiemle, D.; *Spectrometric Identification of Organic Compounds*, 8<sup>th</sup> ed.; John Wiley & Sons: New York, 2014.
48. Santos-Magalhães, N. S.; Pontes, A.; Pereira, V. M. W.; Caetano, M. N. P.; *Int. J. Pharm.* **2000**, *208*, 71. [Crossref]
49. Zili, Z.; Sfar, S.; Fessi, H.; *Int. J. Pharm.* **2005**, *294*, 261. [Crossref]
50. Ma, J.; Feng, P.; Ye, C.; Wang, Y.; Fan, Y.; *Colloid Polym. Sci.* **2001**, *279*, 387. [Crossref]
51. Joo, H. H.; Lee, H. Y.; Guan, Y. S.; Kim, J. C.; *J. Ind. Eng. Chem.* **2008**, *14*, 608. [Crossref]
52. Moinard-Chécot, D.; Chevalier, Y.; Briançon, S.; Beney, L.; Fessi, H.; *J. Colloid Interface Sci.* **2008**, *317*, 458. [Crossref]
53. Tekade, R. K.; *Biomaterials and Bionanotechnology*; Elsevier: London, UK, 2019.
54. Nimmerjahn, A.; Kirchhoff, F.; Kerr, J. N. D.; Helmchen, F.; *Nat. Methods* **2004**, *1*, 31. [Crossref]
55. Wang, X.; Lou, N.; Xu, Q.; Tian, G. F.; Peng, W. G.; Han, X.; Kang, J.; Takano, T.; Nedergaard, M.; *Nat. Neurosci.* **2006**, *9*, 816. [Crossref]
56. Schnell, C.; Shahmoradi, A.; Wichert, S. P.; Mayerl, S.; Hagos, Y.; Heuer, H.; Rossner, M. J.; Hülsmann, S.; *Brain Struct. Funct.* **2013**, *220*, 193. [Crossref]

Submitted: May 16, 2022

Published online: October 19, 2022

